Temporal and Spatial Organization of Chemical and Hydrodynamic Processes. The System Pb^{2+}−Chlorite−Thiourea

Vladimir V. Udovichenko,[†] Peter E. Strizhak,*[,†] Agata Toth,[‡] Dezso Horwath,[‡] Steven Ning,[§] and Jerzy Maselko[§]

L.V. Pysarzhevsky Institute of Physical Chemistry, National Academy of Sciences of Ukraine, pr. Nauki 31, Kiev, 03039, Ukraine, Department of Physical Chemistry, University of Szeged, Hungary, and Department of Chemistry, University of Alaska, Anchorage, 3211 Providence Drive, Anchorage, Alaska 99508-8108

Received: January 30, 2008; Revised Manuscript Received: March 4, 2008

Precise spatio-temporal organization of chemical, hydrodynamic, and mechanical processes is typical for biological systems where particular chemical reactions have to accrue in precisely assignment place and time. It is rarely studied and observed in chemical systems. We report unusual precipitation pattern formation of $PbSO_4$ in chemical media (Pb^{2+}−Chlorite−Thiourea System). We have found that there is a region in a plane of initial concentrations of chlorite ions and thiourea where precipitation of lead sulfate appears in a form of ring if a pellet of lead nitrate is placed into the system. The whole process may be divided into three stages: movement of first circular front of lead containing solution, formation of a ringlike pattern of lead sulfate, and finally, propagation of this pattern resulting in a formation of ring with final inside diameter. Our experiments indicate that the following values are reproducible and quantify the $PbSO_4$ ring evolution: induction time, radius of the ring birth, speed of ring propagation toward the center, and final inside radius of the ring. Numerical solution of kinetic equations allowed us to give a qualitative explanation for the phenomenon observed. Formation and evolution of the $PbSO_4$ rings are caused by interplay of concentration gradients in the system and chemical reactions that occur in excitable chlorite−thiourea system. Chemical reactions and hydrodynamic processes form a complex causal network that made morphogenesis of this unusual pattern possible.

Introduction

In the process of biological morphogenesis, the incredibly complex (from a point of a view of a chemist) structures are self-constructing. With respect to this problem, a lot of studies have been performed regarding pattern formation and evolution that actually shows how diffusion-driven instability may be responsible for biological morphogenesis.[1–4] As a result, the precise spatio-temporal organization in biological morphogenesis seems to be controlled by the complex casual network of the chemical, hydrodynamic, and mechanical processes. However, this kind of complex morphogenesis, in which the chemical, hydrodynamic, and mechanical processes take place, has not yet been the subject of intensive experimental studies in chemical systems.

During past decades, various spatial patterns have been found in different chemical systems.[5–10] Formation of traveling waves, mosaic patterns, spots, strips, etc., have been observed in homogeneous solutions and electrochemical systems as well as in heterogeneous catalytic reactions. Numerous examples demonstrate the spatial patterns formation associated with various precipitation processes. Particularly, in the excitable or oscillating chemical systems, precipitation has been observed in a few cases. In the first case, it occurs as the precipitation of an intermediate or a product of the reaction. For instance, the MnO_2 precipitation in the permanganate chemical oscillator[11–13] and the sulfur precipitation in the Cu(II) catalyzed reaction between H_2O_2 and KSCN.[14] Another example is represented by the CuS fractal thin film formation during the Cu(II)-catalyzed oxidation of ascorbic acid by air oxygen in the presence of Cu(II) coordination compound and sulfide ions in a Petri dish.[15] In second case, the oscillating or excitable chemical system has been perturbed by metal ions that may precipitate because of its reaction with an intermediate or a product of the reaction. A number of publications have been dedicated to silver bromide precipitation in the Belousov−Zhabotinskyi (BZ) reaction perturbed by silver ions.[16–19] Another example is given by inhomogeneous $BaSO_4$ precipitation patterns observed in the excitable chlorite−thiourea−barium chloride reaction system.[20] The wavefront is formed in this system and $BaSO_4$ then precipitates in the region behind the front. In this system formation of patterns is related to the interaction of the chemical precipitation with hydrodynamics that is caused by the changed in density of the solution due to the exothermic chemical reactions. The interaction of chemical reactions with hydrodynamics have been studied in the polymerization systems[21,22] and in "chemical garden" reactions.[23,24]

However, in all these cases, except the CuS fractal film formation,[15] precipitations either appeared just as a nonappreciable consequence of nonlinear chemical reaction or have been used to highlight reaction mechanism or wavefront propagation. Therefore, little is known about spatial patterns observed if precipitation is coupled to excitable or oscillating chemical system.

In this work, we demonstrate formation and evolution of a ring of the $PbSO_4$ precipitation in excitable chemical media capable to produce sulfate ions. For this purpose we have studied

* Corresponding author. Tel./Fax: (38044) 265 66 63. E-mail: pstrizhak@hotmail.com.
[†] National Academy of Sciences of Ukraine.
[‡] University of Szeged.
[§] University of Alaska.

10.1021/jp8009063 CCC: $40.75
Published on Web 04/22/2008

TABLE 1: Rate Laws and Rate Constants for the Mechanism of Chlorite−Thiourea Reaction

reaction	rate law	rate constant
R1[25]	$k_1[ClO_2^-][SC(NH_2)_2][H^+]$	10.5 M^{-2} s^{-1}
R2[26]	$k_2[ClO_2^-][HOCl][H^+]$	1.12×10^6 M^{-2} s^{-1}
R3[26]	$k_3[Cl_2O_2][SC(NH_2)_2]$	2×10^5 $M^{-1}s^{-1}$
R4[26]	$k_4[HOCl][SC(NH_2)_2]$	1×10^4 M^{-1} s^{-1}
R5[25]	$k_5[Cl^-][HOCl][H^+]$ $k_{-5}[Cl_2(aq)]$	$k_5 = 1.8 \times 10^4$ M^{-2} s^{-1}; $k_{-5} = 11$ s^{-1}
R6[27]	$k_6[ClO_2^-][Cl_2O_2]$	2×10^5 M^{-1} s^{-1}
R7[25]	$k_7[ClO_2^-][HOCl][H^+]$	1.06×10^6 M^{-2} s^{-1}
R8[25]	$k_8[ClO_2^-][HOSC(NH)NH_2]$	7.5×10^2 M^{-1} s^{-1}
R9[25]	$k_9[ClO_2(aq)][HOSC(NH)NH_2]$	5×10^3 $M^{-1}s^{-1}$
R10[29]	$k_{10}[ClO_2^-][HO_3SC(NH)NH_2]$	2.0 ± 0.5 M^{-1} s^{-1}
R11[29]	$k_{11}[HOCl][HO_3SC(NH)NH_2]$	25 ± 7 M^{-1} s^{-1}

the chlorite−thiourea reaction, which is known as a bistable system.[25–29] The $PbSO_4$ precipitation is studied by varying the initial concentrations of thiourea, chlorite and chloride ions as well as changing acidity. To verify possible chemical reasons for the phenomenon observed, we have also studied system behavior by perturbing it in several ways during the induction time.

Chlorite−Thiourea Reaction

Nonlinear phenomena observed in this reaction as well as its kinetics and mechanism have been studied during the past decade.[25–30] In a continuously stirred flow tank reactor (CSTR), this reaction exhibits periodic and chaotic oscillations. In batch, it shows clock reaction behavior or single pH oscillation depending on the initial conditions. In a spatially distributed system, e.g., if the chlorite−thiourea reaction runs in a Petri dish, it produces chemical waves exhibiting features of excitable chemical media.

Chlorite oxidizes thiourea in acidic or neutral media, producing sulfate and urea. The reaction is highly exothermic, with the theoretical enthalpy change being -1.17×10^3 kJ mol^{-1}.[20] At values of pH >3 the stoichiometry was found to be[25]

$$2ClO_2 + SC(NH_2)_2 + H_2O \rightarrow SO_4 + CO(NH_2)_2 + 2Cl^- + 2H^+ \quad (1)$$

The suggested chlorite-based[26] and sulfur(II)-based[27] general models successfully demonstrate that there are two nonlinear driving forces, which could lead to the exotic phenomena that are observed. However, the range of initial reagent concentrations used in present work and observed features of the system behavior make the chlorite-driven mechanism preferable in this case. The whole reaction kinetics may be subdivided into the following four processes:

(1) Initiation:

$$ClO_2^- + SC(NH_2)_2 + H^+ \rightarrow HOSC(NH)NH_2 + HOCl \quad (R1)$$

This reaction is known as the slow and rate-determining step during the initial silent period.[25,26]

(2) Autocatalysis

$$HOCl + ClO_2^- + H^+ \rightarrow Cl_2O_2 + H_2O \quad (R2)$$

$$Cl_2O_2 + SC(NH_2)_2 + H_2O \rightarrow 2HOCl + HOSC(NH)NH_2 \quad (R3)$$

These two reactions represent an autocatalytic cycle where HOCl is an autocatalytic species whose diffusion controls the rate of wave propagation.[26,28] An intermediate Cl_2O_2 must be very reactive and it can rapidly react with the substrate,[26] so R2 seems to be slower and rate-determining step in the autocatalytic production of HOCl. Observed acceleration of the reaction by increasing chlorite ions concentration and acidity or decreasing the concentration of thiourea[28] confirms this assumption. The substrate represented by thiourea may also be sufenyl, sulfinic, or sulfonic acid as well.

The autocatalytic loop is caused by the reactions of the hydrogen ion as is indicated by reactions 1 and R1.

(3) Inhibition:

$$HOCl + SC(NH_2)_2 \rightarrow HOSC(NH)NH_2 + H^+ + Cl^- \quad (R4)$$

$$HOCl + Cl^- + H^+ \rightarrow Cl_2 + H_2O \quad (R5)$$

$$Cl_2O_2 + ClO_2^- \rightarrow 2ClO_2 + Cl^- \quad (R6)$$

$$HOCl + 2ClO_2^- + H^+ \rightarrow 2ClO_2 + Cl^- + H_2O \quad (R7)$$

R4 appears to be an important component of the process able to control the autocatalytic cycle.[27] R5 also may account for this because of the elimination of HOCl. R6 and R7 are responsible for the chlorine dioxide formation, and the significance of these reactions arises at the final stages of the process after all the thiourea has been consumed.[25,28] Namely, the green wave of chlorine dioxide is observed visually if the reaction runs in a Petri dish. A chlorine dioxide wave is formed spontaneously in acidic media if the ratio of initial concentrations of chlorite to thiourea is at least 2.[20,28] If the value of this ratio is below unity, the reaction mixture becomes unexcitable.[26]

(4) Further oxidation of sulfenyl acid and sulfate production:

$$ClO_2^- + HOSC(NH)NH_2 \rightarrow HO_3SC(NH)NH_2 + Cl^- \quad (R8)$$

$$2ClO_2 + HOSC(NH)NH_2 + H_2O \rightarrow HO_3SC(NH)NH_2 + HOCl + H^+ + Cl^- \quad (R9)$$

$$ClO_2 + HO_3SC(NH)NH_2 + H_2O \rightarrow SO_4^{2-} + CO(NH_2)_2 + HOCl + H^+ \quad (R10)$$

$$HOCl + HO_3SC(NH)NH_2 + H_2O \rightarrow SO_4^{2-} + CO(NH_2)_2 + Cl^- + 3H^+ \quad (R11)$$

It is generally accepted[28,29] that because of the stability of sulfonic acid oxidation of sulfenyl to sulfonic acid (R8, R9) is relatively easy. This step is followed by the slower oxidation of sulfonic acid (R9, R10), resulting in a sharp pH decrease and simultaneous production of sulfate ions.[25,30]

Rate laws and the values of rate constants for elementary steps suggested to describe the kinetics of the chlorite−thiourea reaction are collected in Table 1. In this paper, we are considering a mostly qualitative model without taking into account critical analysis of the reaction rate constants and reaction pathways. The more comprehensive study is beyond this paper. From one hand, that study should take into account critical evaluation of rate constants based on sensitivity analysis and, on the other hand, should consider other kinetic studies of the chlorine-species kinetics presented in literature.[32,33]

Formation and movement of the chemical front can be understand by considering perturbation of the system that is causing reaction 1 to be completed in the place of perturbation. Next, the hydrogen ion diffuses from the point of perturbation

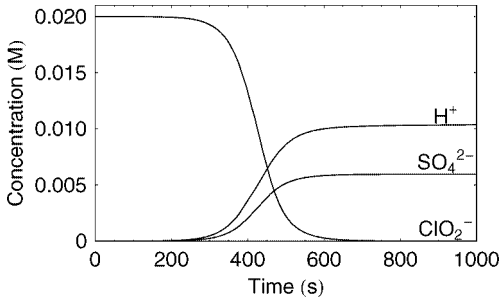

Figure 1. Kinetics curves for the presented model. Initial concentrations: $[ClO_2^-] = 0.02$, [TU]= 0.018, pH 6.2, $[Cl^-] = 0.0135$.

and according to reaction R1 initiates the chain of reactions. The process is then repeated, forming the moving reaction front.

Differential equations representing the kinetic mechanism and rate constant presented inn Table 1 have been solved and results are presented in Figure 1. Kinetics curves are typical for system that produces chemical front. The initiation time is about 400 s. Before initiations, concentrations represent the solution before a front. After initiation, the solution after the front is represented. The substantial increase of SO_4^{2-} is observed that allows the $PbSO_4$ precipitation. Similarly, the increase in hydronium ion concentration allows diffusion before the front and reaction initiation.

Experimental Section

All reagents used, except sodium chlorite, were of analytical grade (Aldrich). Sodium chlorite (Aldrich) was used without purification. It contains 80 ± 1% sodium chlorite determined by an iodometric method. The major impurity (20%) was sodium chloride, which has been determined by standard procedure.[34] Stock solutions of 0.225 M thiourea and 0.45 M sodium chlorite were prepared using doubly distilled water. Sodium chlorite solutions were prepared just before use.

An excitable reaction mixture was prepared by mixing appropriate volumes of stock solutions in the following sequence: thiourea, sodium chloride, sodium chlorite. Initial concentrations of reagents have been varied in the following ranges: $[\text{thiourea}]_0 = 0.002-0.06$ M, $[ClO_2^-]_0 = 0.002-0.1$ M. An appropriate amount of a 1.0 M solution of sodium chloride has been added to the reaction system to keep a constant initial concentration of sodium chloride in the reaction mixture (0.0135 M). In some experiments, the initial concentration of sodium chloride was varied in the range of 0.0135−0.04 M.

The pH of solutions was monitored by pHmeter (Fisher Scientific). The solutions were not buffered. The initial pH of the reaction mixture was always 6.2 if $HClO_4$ was not additionally added into reaction mixture. The pH of the reacted solution, monitored after 10 min of mixing all reagents, has been found in a region of pH 3−4 depending on the initial concentration of chlorite ions. In some experiments, an appropriate amount of $HClO_4$ was added to change acidity in the initial concentration range of 0−1 M. The volume of a reaction mixture was always 300 mL. All experiments have been performed at the initial temperature $T = 20 \pm 0.5$ °C.

After mixing of all reagents, the reaction mixture was placed into a square-shaped glass bath with size 248 × 248 mm^2. Our experiments have indicated that in this case there was no boundary effect on the patterns formed. Reaction has been initiated by placing a pellet of $Pb(NO_3)_2$ (diameter = 6 mm, height = 3 mm) into the center of the bath. Pellets have been prepared using a Perkin-Elmer press. There is no effect of the pellet size on phenomena observed if the pellet weight is inside the range of 0.2−0.6 g. In all experiments reported here, we have used the pellet of 0.4 g. There is no effect of time delay between excitable mixture preparation and adding the pellet on the induction time or other characteristics of the precipitation pattern if the delay is less than 5 min.

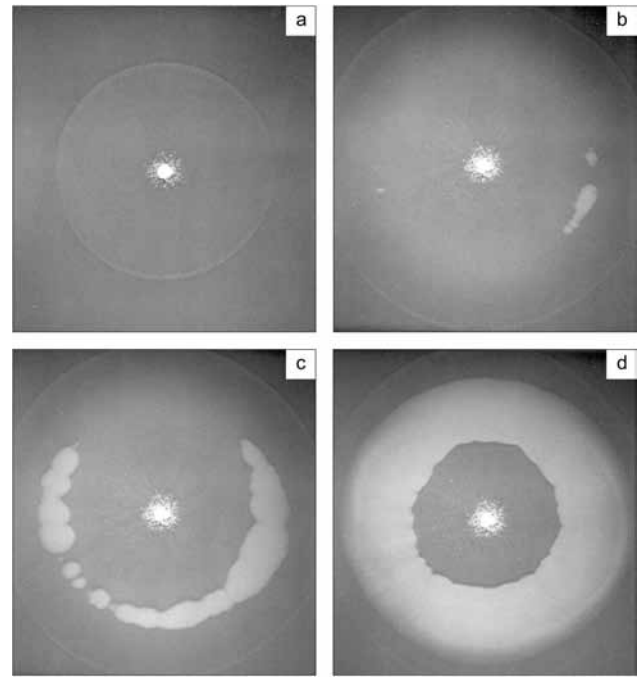

Figure 2. Frames showing system evolution after adding the $Pb(NO_3)_2$ pellet: (a) development of the ring of heavy lead chlorite containing solution, $t = 210$ s; (b) spots of $PbSO_4$, $t = 660$ s; (c) $PbSO_4$ ring formation, $t = 675$ s; (d) final $PbSO_4$ ring after finishing its propagation, $t = 720$ s. Initial concentrations: $[\text{thiourea}]_0 = 0.018$ M, $[ClO_2^-]_0 = 0.03$ M, $[Cl^-]_0 = 0.0135$ M.

Results and Discussion

Formation of Precipitation Pattern. Our experiments have shown that placing the $Pb(NO_3)_2$ pellet into chlorite−thiourea excitable media initiates formation and evolution of precipitation pattern as shown in Figure 2.

The whole process may be divided into three stages. At the first stage, a $Pb(NO_3)_2$ pellet dissolves and visible circle propagates from the center as shown in Figure 2a. This circle is formed by a heavy lead-containing solution that is located at the bottom of the reaction mixture. It contains dispersed particles of lead chlorite that appear because of the reaction between lead nitrate and chlorite ions, which results in lead chlorite precipitation. It was found that similar circle propagation is observed if $Pb(NO_3)_2$ pellet is placed into solution containing sodium chlorite only. On the contrary, no visual circle formation has been observed in solutions of sodium chloride or thiourea. The circle propagates until it reaches the boundary of the bath in such a way that square of its radius is proportional to the time of evolution as it shown in Figure 3. This plot represents only the heavy bottom solution. A slope for dependence presented in Figure 3 gives a high value of the mass transfer coefficient (0.208 ± 0.004 cm^2 s^{-1}). It indicates either an autocatalytic or convective nature of the circle propagation.

During outer circle propagation the upper solution moves toward the center. In our experiment the total height of the solution was 11 mm and the bottom solution height was about 1 mm. Therefore we may assume that the movement of the

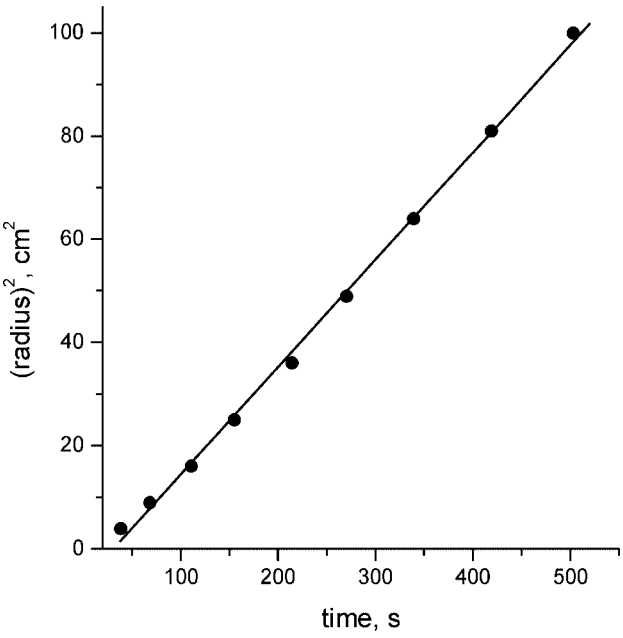

Figure 3. Dependence of squared radius of lead chlorite circle formed at various initial conditions on the time of its evolution.

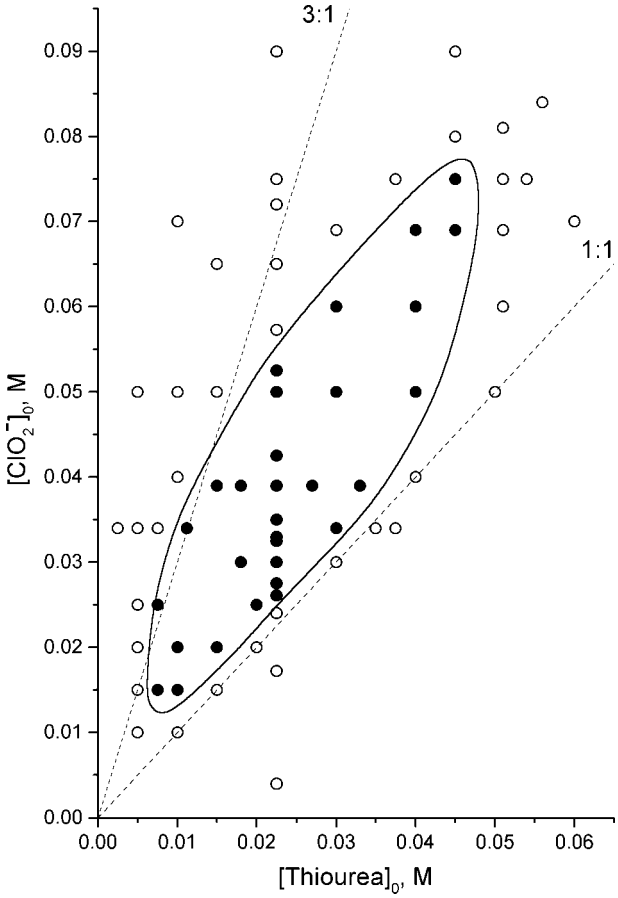

Figure 4. Phase diagram in the plane $[ClO_2^-]_0$−$[thiourea]_0$ illustrating the region of initial conditions where the ring-formation occurs (filled dots) and does not occur (open dots).

upper solution toward the pellet was 10 times slower then the movement of the lower solution.

After induction period precipitation of $PbSO_4$ starts in a form of spots located at certain distance from the center as shown in Figure 2b. These spots propagate rapidly with speed in the range

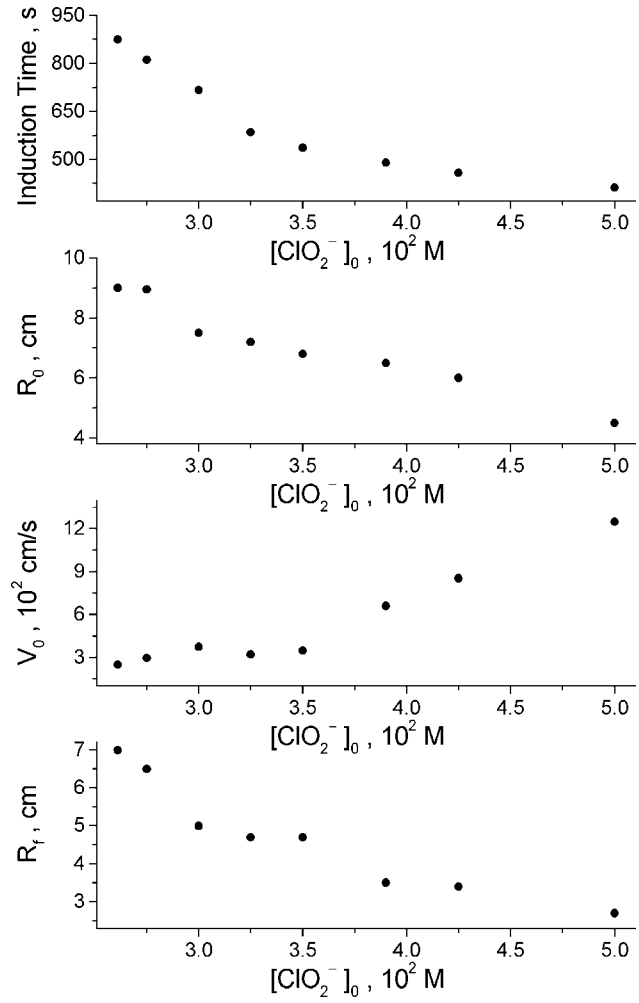

Figure 5. Dependencies of induction time, R_0, V_0, and R_f on the initial concentration of chlorite ions. Other initial conditions are fixed: $[thiourea]_0 = 0.0225$ M, $[Cl^-]_0 = 0.0135$ M.

of 5 − 20 cm/s. The speed of propagation does not depend on the direction. During a short time interval (1−5 s) these spots appear everywhere forming a ring shown in Figure 2c. This ring is always located inside the initial circle formed by a heavy solution of lead chlorite.

During the third stage, this ring propagates in both radial directions. In the beginning it moves faster toward the center and slower outside. At certain moment of time this propagation toward the center slows down and stops forming the final ring with certain inside diameter. This final ring is shown in Figure 2d. Figure 2d illustrates that although the outer ring is almost a perfect circle, the inner ring shows a slightly octagonal pattern. All three stages of the precipitation pattern evolution appear at the bottom of the solution.

Phase Diagram. The formation of the precipitation pattern depends on the initial concentration of chlorite ions ($[ClO_2^-]_0$) as well as the initial concentration of thiourea ($[thiourea]_0$). Figure 4 gives the phase diagram in the plane $[ClO_2^-]_0$−$[thiourea]_0$.

It follows from the data presented in Figure 4 that the $PbSO_4$ ring is observed within the region of ratio $[ClO_2^-]_0/[thiourea]_0$ values from 1 to 3, i.e., there exist upper and lower limits for the pattern formation.

Formation of the $PbSO_4$ ring is accompanied by the appearance of green wave of chlorine dioxide. We have not observed a formation of the green wave if $[ClO_2^-]_0/[thiourea]_0 < 1$. As

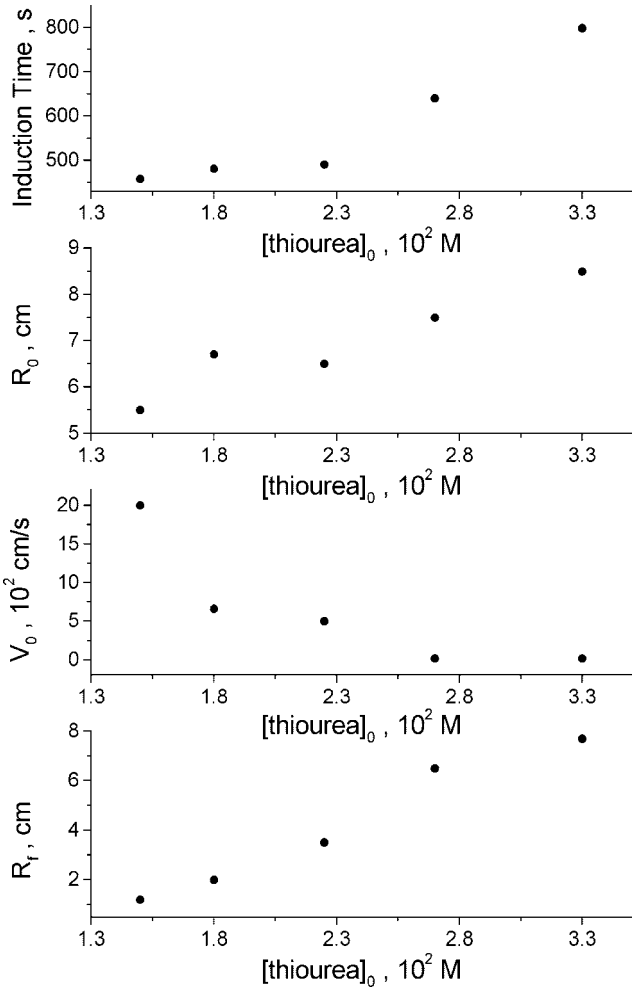

Figure 6. Dependencies of induction time, R_0, V_0, and R_f on the initial concentration of thiourea. Other initial conditions are fixed: $[ClO_2^-]_0 = 0.039$ M, $[Cl^-]_0 = 0.0135$ M.

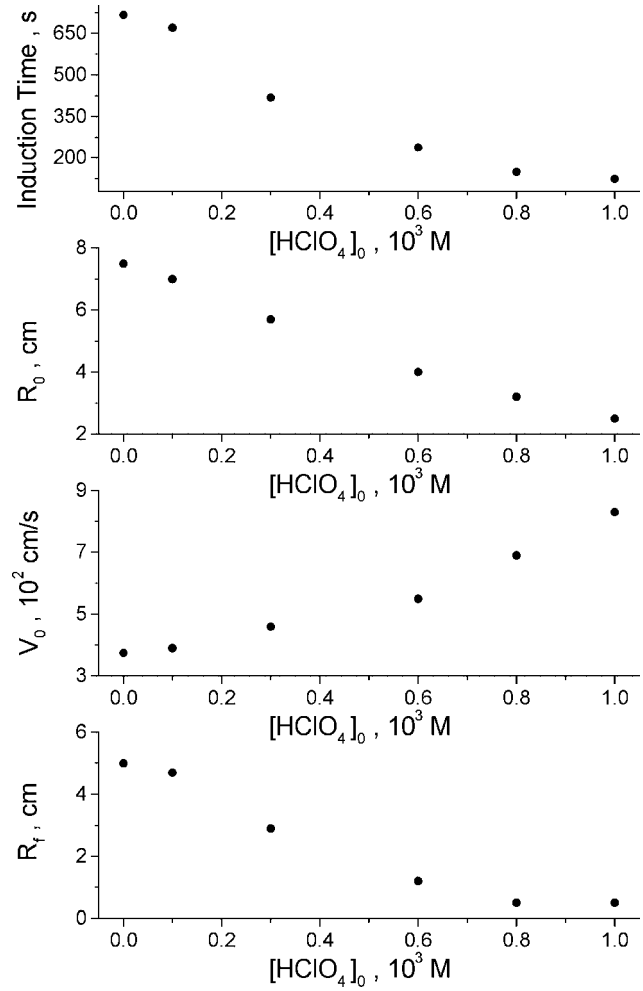

Figure 7. Dependencies of induction time, R_0, V_0 and R_f on the initial concentration of $HClO_4$. Other initial conditions are fixed: $[\text{thiourea}]_0 = 0.0225$ M, $[ClO_2^-]_0 = 0.03$ M, $[Cl^-]_0 = 0.0135$ M.

a result, there is no $PbSO_4$ precipitation at all, i.e., the reaction does not occur. At $[ClO_2^-]_0/[\text{thiourea}]_0 > 3$, our experiments indicate that the green wave of chlorine dioxide formed very rapidly and unpredictably. This leads to the absence of $PbSO_4$ ring formation. Contrary, $PbSO_4$ precipitation appears everywhere randomly. This is also the case for high initial concentration of both reagents.

Quantification of Ring Formation and Evolution. We have found that the following values may be used for a quantification of the $PbSO_4$ ring formation and evolution: induction time, radius of ring formation (R_0), and initial speed of ring propagation toward the center (V_0), final inside diameter of the ring (R_f). The induction time is reproducible with accuracy of 5 s, and the values of R_0 and R_f are reproducible with an accuracy of 3 mm. Figure 5 gives dependencies of these quantities on the initial concentration of chlorite ions.

An increase in $[ClO_2^-]_0$ causes a decrease in induction time and initial and final ring radii. Contrary, the speed of ring propagation increases.

Shown in Figure 6 are the dependencies of the same quantities on the initial concentration of thiourea.

All these dependencies are characterized by opposite character comparing to those for the chlorite ions. Namely, the values of induction time, R_0, and R_f increase with an increase in initial thiourea concentration, whereas the speed of ring propagation decreases.

We have also studied dependencies of these quantities on acidity by adding various amount of $HClO_4$ to the reaction mixture. The data shown in Figure 7 indicate that an increase in acidity leads to the similar effect as an increase in chlorite ions concentration.

Dependencies of these quantitative values on initial concentrations of reagents obviously indicate that acceleration of the reaction caused by increase either of initial chlorite concentration and acidity or by decrease of thiourea concentration[29] makes shorter induction time and radii where ring is born and stopped. Contrary, the speed of ring propagation increases with an increase in reaction rate. Moreover, we have found that the difference between R_0 and R_f is always constant within the precision of measurements of these values: $\Delta R = R_0 - R_f = 2.4 \pm 0.5$ cm.

The effect of chloride ions on the precipitation pattern evolution also has been studied. An increase in the induction time and radius of ring birth with an increasing of the initial chloride concentration indicate that chloride ions decelerate the reaction, as illustrated at Figure 8.

Perturbation of the System during Induction Time. Our studies show that if the $Pb(NO_3)_2$ pellet is not placed in the system than shaking of the solution or touching it with hot needle causes an appearance of green wave of chlorine dioxide. Moreover, placing a pellet of $AgNO_3$ or $Hg_2(NO_3)_2$ immediately initiate a green wavefront propagating from the pellet. If lead

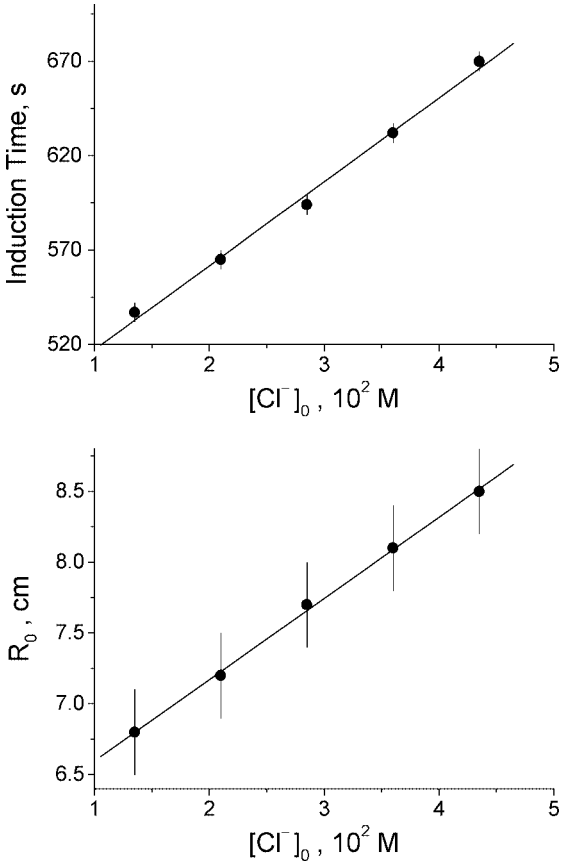

Figure 8. Dependencies of induction time and R_0 on the initial concentration of chloride ions. Other initial conditions are fixed: $[\text{thiourea}]_0 = 0.0225$ M, $[ClO_2^-]_0 = 0.035$ M. Error bars for induction time correspond to standard deviation obtained in 6 independent experiments. Error bars for R_0 correspond to the soft edges of precipitation ring obtained in six independent experiments.

TABLE 2: Examples of Concentrations of Important Chemicals

species	lower solution	upper solution
$[ClO_2^-]$	1.8×10^{-4} M	0.03 M
[TU]	1×10^{-3} to 1×10^{-2} M	0.018 M
$[Pb^{2+}]$	<0.17 M	>0
pH	4.0	6.2

ions are present in a solution, the wave is accompanied by $PbSO_4$ precipitation that appears similar to the $BaSO_4$ precipitation reported previously.[20] The introduction of lead ions in a form of $PbCl_2$ pellet initiates formation and evolution of lead sulfate precipitation pattern similar to that induced by $Pb(NO_3)_2$ pellet. Placing a pellet of $Pb(ClO_2)_2$ or $Ba(NO_3)_2$ into reaction mixture does not affect essentially the chlorite−thiourea system. In this case, there is no certain induction time and the reaction starts stochastically.

Discussion

The chlorite−thiourea system is excitable if $[ClO_2^-]_0/[\text{thiourea}]_0 > 1$,[26] and this condition of the system excitability governs the concentration limit of the $PbSO_4$ ring formation. The appearance of the chlorine dioxide wave indicates that system has been ignited and autocatalysis has been started according to reactions R2 and R3. It results in a release of sulfate ions into solution. If lead ions are presented in a solution, precipitation of lead sulfate occurs.

Adding the $Pb(NO_3)_2$ pellet disturbs the chlorite−thiourea system in two ways. First of all, it causes appearance of the concentration gradient of lead ions in a solution that induces concentration gradients, both vertical and horizontal, of the components of the chlorite−thiourea reaction. Lead ions are involved in a reaction of lead chlorite formation as well as the formation of complexes with thiourea or chloride ions

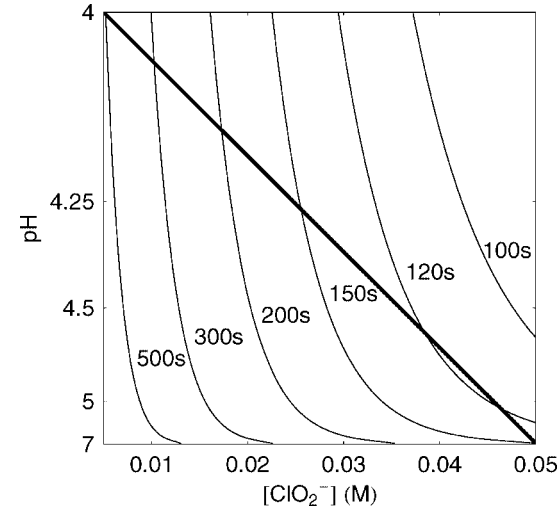

Figure 9. Dependence of the induction time from the pH and chlorite ion concentration.

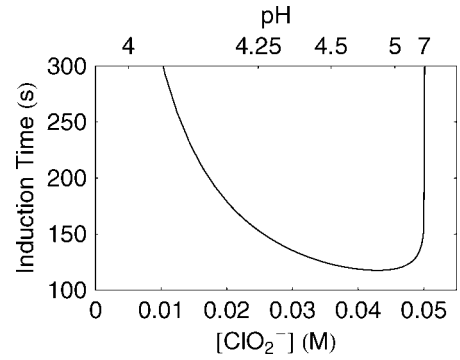

Figure 10. Dependence of the induction time as a function of chlorite ion and pH concentration. The concentration values for a ClO_2^- are on the lower horizontal axis and pH is on the upper horizontal axis.

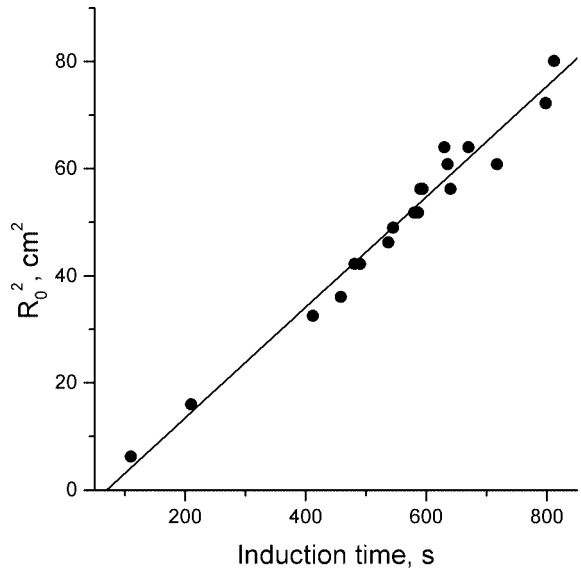

Figure 11. Dependence of R_0^2 on induction time for the $PbSO_4$ rings formed at various initial conditions.

$$Pb^{2+} + 2ClO_2 \rightleftarrows Pb(ClO_2)_2 \quad (2)$$

$$Pb^{2+} + n\text{thiourea} \rightleftarrows Pb[\text{thiourea}]_n^{2+} \quad (3)$$

$$Pb^2 + nCl^- \rightleftarrows [PbCl_n]^{2-n} \quad (4)$$

where $n = 1-4$.

Among all products of these reactions, the lead chlorite is characterized by lowest solubility and highest stability. Solubility product constant of lead chlorite is equal to 5.55×10^{-9} M^3 that we have estimated from its solubility in water solutions (0.095 g/100 mL).[34] For comparison, the solubility product constant of lead sulfate is equal to 1.82×10^{-8} M^2.[34] Therefore, the lead chlorite precipitates under conditions of experiments reported in this paper. The solubility of $PbCl_2$ in water is 0.99 g/100 mL[34] and it does not precipitate under these conditions. Complexes of lead with thiourea or chloride ions are characterized by low values of stability constants. Logarithms of the stability constants for the lead complexes with thiourea are in the range of 0.6−2.04 and for lead complexes with chloride ions are in the range 1.3−1.8 depending on the value of coordinated molecules.[35] Therefore, reaction 2 significantly reduces the chlorite ions concentration whereas reactions 3 and 4 slightly decrease concentrations of thiourea and chloride ions in the reaction mixture. In addition, the lead undergoes hydrolysis, increasing the concentration of the hydronium ion.

Second, placing the $Pb(NO_3)_2$ pellet introduces heterogeneities into the system. These heterogeneities may serve as centers of the birth of autocatalytic wave of chlorine dioxide as have been shown by disturbing the system by silver or mercury nitrate pellet.

Finally, dissolution of lead nitrate pellet in the reaction mixture and reactions 24 result in the formation of a heavy solution with particles of lead chlorite and its propagation from the center (Figure 2a). Spreading of this solution is governed by viscous damping,[36] in agreement with the proportionality of the square of the solution radius to the time of its evolution (Figure 3). The lower solution moves out of the pellet and the upper solution moves toward the pellet. Between them must be a solution that does not move. The movement of the lower solution is about 10 times faster them the movement of the upper solution.

In our experiment, we observe two emergent phenomena that are very unusual. The first is the initiation of the spreading chemical waves and is related to its precipitation of lead sulfide. It appears in the middle of the $Pb(ClO_2)_2$ solution far from the pellet and far from the end of the lead solution that has the longest time since exposure to the pellet. The appearance of the waves appears in few points in a very well defined ring (look at images b and c in Figure 2). This well-defined ring suggests that it is related to chemical kinetics but not to the formation of lead chlorite precipitation. This ring formation should be explained with the interesting properties of the hydrogen ion. In the lead solution close to the pellet and on the bottom, the concentration of the H^+ is relatively high because of the hydrolysis of the lead. Taking into considerations most of the equilibrium, we have calculated pH as equal to 4.0. In the upper solution, the pH has been measured as 6.2.

Table 2 indicates that chlorite ion and thiourea compounds will diffuse in vertical direction from upper solution to lower solution, whereas the hydronium ion will diffuse in opposite directions.

All these ions influence the initiation time; for pH and chloride, it is presented in Figures 9 and 10. Going vertically from upper to lower solution, the concentration of the pH and

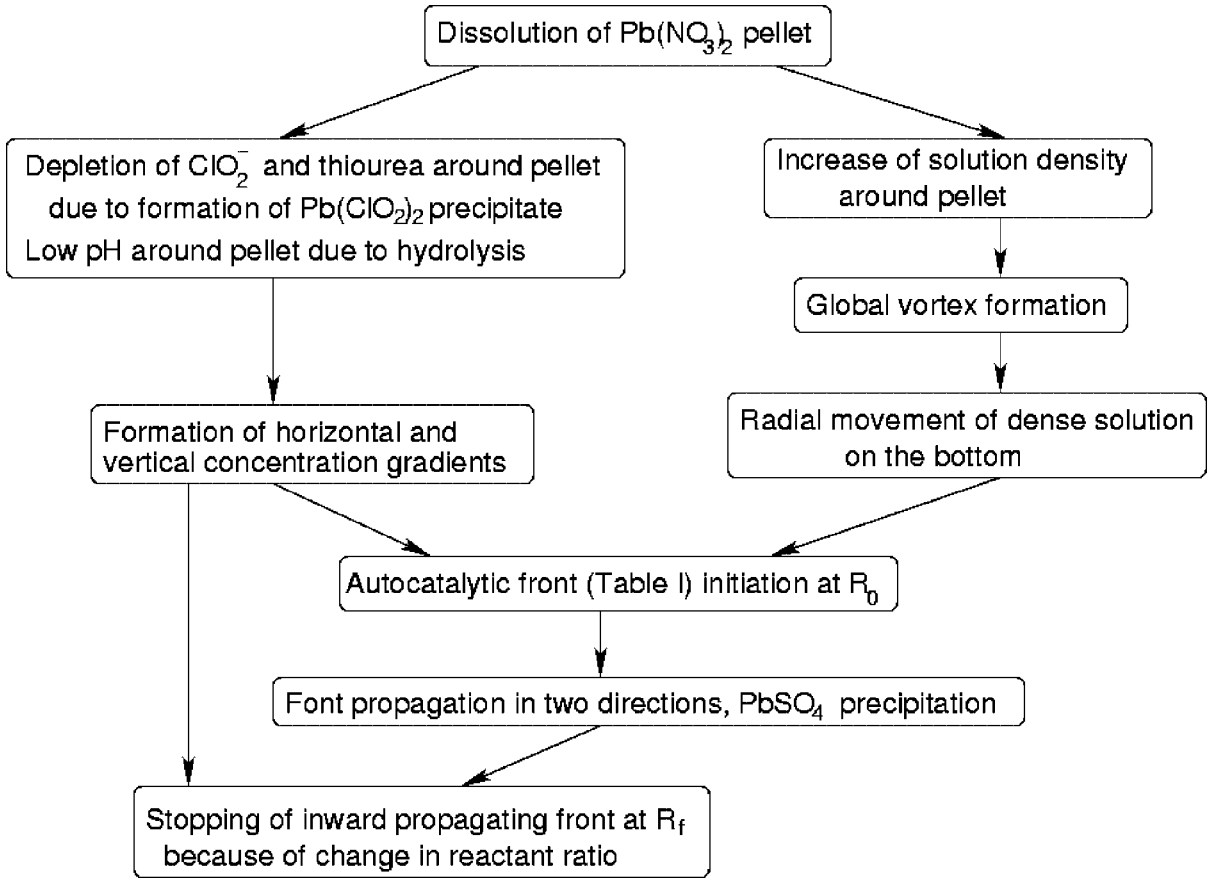

Figure 12. Schematic representation of the causal processes network controlling precipitation ring formation.

chloride ions will decrease continuously. Similarly, because of constant diffusion, these concentrations in the lower solution will increase continuously with increasing distance from the pellet. These vertical diffusions will also create horizontal gradients in both lower and upper solutions.

Solving kinetic equations representing kinetic mechanism presented inn Table 1 we obtained dependence of the induction times on pH and chlorite ion concentration, as presented in Figure 9.

Figure 9 indicates that the induction time will have a minimum. Detailed values of these concentrations as a function of radius are not known but in the case of the linear change, as is presented by a fat line in Figure 9, this minimum is presented in Figure 10.

According to Figure 10, the minimum value for the initiation time where the formation of the wave will appears in the middle of the solution was observed experimentally.

Another unusual phenomena is the stopping of the moving front at the position of R_f. As we observed, the precipitation ring was formed in the lower solution. Therefore, it must be assumed that the wave movement was in the lower solution, between the lower and upper solution, or in the lower part of the upper solution. We may assume that far from the pellet, because of vertical diffusion, the concentrations in the lower solution will be equal to the concentrations in the upper solution. According to Table 2, the ratio of $[ClO_2^-]$/[TU] close to the pellet is 0.18−0.018, whereas far from the pellet maybe be greater than 1. Concentrations of chlorite and thiourea intersecting each other at certain distance from the center R_f. Therefore, at $R < R_f$, the wave of chlorine dioxide can not propagate and stops because the system is not excitable. Interesting scaling behavior is presented in Figure 11. The R^2_0 is a linear function of induction time measured for different initial concentrations of chlorite and thiourea concentrations. It will be trivial if the precipitation will begin in the edge of the spreading solution according. Figure 11 suggests that it is a delay in the process of front initiation caused by first depletion and next regeneration of chlorite, hydronium, and thiourea concentrations. In this paper, we are presenting mostly qualitative model observed phenomena. The detailed quantitative model is beyond the scope of this discovery paper.

It is worth noting that scattering of points around the line in Figure 11 increases with an increase in the induction time. This result corresponds to observed degradation of the induction time reproducibility of the chlorite−thiourea reaction at low values of the $[ClO_2^-]_0$/[thiourea]$_0$ ratio.[25]

In summary, we may conclude that quantitative parameters that characterize the ring birth and evolution depend on the rate of autocatalytic step of the reaction. Particularly, a decrease in induction time, radii of ring birth and halt, and corresponding increase in the speed of ring propagation are caused by acceleration of the autocatalytic step. An increase in chlorite ion concentration or acidity may account for this via reactions R1 and R2.[26,28] Contrary, an increase in initial concentration of thiourea causes the opposite effect because of inhibition of the autocatalytic step due to the R4 reaction.[26] The suppressing effect of chloride ions in simplest consideration may be explained by elimination of HOCl according to reaction R5.

Conclusion

The formation of the precipitation ring includes at least 22 reactions that are presented in Table 1. In addition, the dissolution reaction and the reaction of the Pb^{2+} with sulfate, chlorite, thiourea, and lead hydrolysis are present. The diffusions of ClO_2^-, H^+ ions, and thiourea are also present. All these diffusions are crucial to pattern formation. The dissolution of lead nitrate causes a density gradient that is the source of the radial hydrodynamic movement, establishment of the global vortex, and the division into lower and upper solution. The hydrodynamic movement interacts with the H^+ ion, chlorite ion, and thiourea diffusion that is further causing chemical wave initiation, propagation, and stopping.

The precipitation ring is characterized by the initiation ring defined by R_0 and the inner radius R_f that is defined by the stopping of the moving front. In biological morphogenesis, it is crucially important that different chemical processes occur in precisely defined spatial positions. The spatio-temporal control of these processes is the source of complex structure self-construction. It is done by complex causal network of chemical, hydrodynamic, and mechanical processes. In our system, we observe a similar mechanism where a causal network of chemical and hydrodynamic processes leads to the control of pattern formation.

This causal network is presented in Figure 12.

Acknowledgment. The work was partially supported by the National Research Council through the Twinning Program supporting scientific collaboration with the Ukraine, the National Science Foundation Grant CHE 0608631, and the Complex System Group, University of Alaska, Anchorage.

References and Notes

(1) Saunders, P. T., Ed.; *Collected Works of A.M. Turing: Morphogenesis*; North Holland: Amsterdam, 1992.
(2) Dulos, E.; Boissonade, J.; Perraud, J. J.; Rudovics, B.; De Kepper, P. *Acta Biotheor.* **1996**, *44*, 249.
(3) Meinhardt H. *Models of Biological Pattern Formation*; Academic Press: New York, 1982.
(4) Lucchetta, E. M.; Lee, J. H.; Fu, L.; Patel, N.; Ismagilov, R. F. *Nature* **2005**, *434*, 1134.
(5) Field, R. J.; Burger, M., Eds.; *Oscillations and Travelling Waves in Chemical Systems*; Wiley−Interscience: Hoboken, NJ, 1985.
(6) Scott, S. K. *Oscillations, Waves, And Chaos in Chemical Kinetics*; Oxford University Press: Oxford, U.K., 1994.
(7) Epstein, I. R.; Showalter, K. *J. Phys. Chem.* **1996**, *100*, 13132.
(8) SchneiderF. W. MünsterA. F. *Nichtlineare Dynamik in der Chemie*; Spektrum Akademischer Verlag: Heidelberg, Germany, 1996.
(9) Epstein, I. R.; Pojman, J. A. *An Introduction to Nonlinear Chemical Dynamics: Oscillations, Waves, Patterns, and Chaos*; Oxford University Press: Oxford, U.K., 1998.
(10) Field, R., Györgyi L., Eds.; *Chaos in Chemical and Biochemical Systems*; World Scientific Press: Singapore, 1993.
(11) Orban, M.; Epstein, I. R. *J. Am. Chem. Soc.* **1990**, *112*, 1812.
(12) Doona, C. J.; Kustin, K.; Orban, M.; Epstein, I. R. *J. Am. Chem. Soc.* **1991**, *113*, 7484.
(13) Melichercik, M.; Sodnomdordz, G.; Treindl, L. *Z. Phys. Chem. (Munich)* **1992**, *175*, 253.
(14) Orban, M. *J. Am. Chem. Soc.* **1986**, *108*, 6893.
(15) Strizhak, P. E. *Chem. Phys. Lett.* **1995**, *241*, 360.
(16) Noszticzius, Z. *J. Am. Chem. Soc.* **1979**, *101*, 3660.
(17) Ruoff, P. *J. Chem. Phys.* **1985**, *83*, 2000.
(18) Kshirsagar, G.; Field, R. J.; Gyorgyi, L. *J. Phys. Chem.* **1988**, *92*, 2472.
(19) Stuk, L.; Roberts, J.; McCormick, W. D.; Noszticzius, Z. *J. Phys. Chem.* **1990**, *94*, 6734.
(20) Hauser, M. J. B.; Simoyi, R. H. *Phys. Lett. A* **1994**, *191*, 31.
(21) Pojman, J. A.; Nagy, I. P.; mSalter, C. *J. Am. Chem. Soc.* **1996**, *115*, 11044.
(22) Pojman, J. A.; Epstein, I. R. *Chaos* **1999**, *9*, 255.
(23) Cartwright, J. H.; Garcia-Ruiz, J. M.; Novella, M. L.; Otalora, F. *J. Colloid Interface Sci.* **2002**, *256*, 351.
(24) Toth, A.; Horvath, D.; Smith, R.; McMahan, J. R.; Maselko, J. *J. Phys. C* **2007**, *490*, 14762.
(25) Epstein, I. R.; Kustin, K.; Simoyi, R. H. *J. Phys. Chem.* **1992**, *96*, 5852.
(26) Rabai, G.; Orban, M. *J. Phys. Chem.* **1993**, *97*, 5935.

(27) Rushing, C. W.; Thompson, C. R.; Gao, Q. *J. Phys. Chem. A* **2000**, *104*, 11561.
(28) Chinake, C. R.; Simoyi, R. H. *J. Phys. Chem.* **1994**, *98*, 4012.
(29) Chinake, C. R.; Simoyi, R. H. *J. Phys. Chem.* **1993**, *97*, 11569.
(30) Gao, Q.; Wang, J. *Chem. Phys. Lett.* **2004**, *391*, 349.
(31) Indelli, A. J. *J. Phys. Chem.* **1964**, *68*, 3027.
(32) Odeh, I. N.; Francisco, J. S.; Margerum, D. W. *Inorg. Chem.* **2002**, *41*, 6500.
(33) Wang, T. X.; Margerum, D. W. *Inorg. Chem.* **1994**, *33*, 1050.
(34) *CRC Handbook of Chemistry and Physics*, 75th ed.; CRC Press: Boca Raton, FL, 1994.
(35) Inczedy, J. *Analytical Applications of Complex Equilibria*; Akademiai Kiado: Budapest, Hungary, 1976.
(36) Perez, E.; Schaffer, E.; Steiner, U. *J. Colloid Interface Sci.* **2001**, *234*, 178.

JP8009063